Biomechanical Modelling of the Femoroacetabular Impingement of the Cam Type

Joana Marta Miguel Lourenço
IST, Universidade de Lisboa, Portugal

November 1, 2013

Abstract

In this study, three-dimensional finite element models based on the specific anatomy of a patient presenting a femoroacetabular impingement of the cam-type are developed. The finite element meshes of the structures of interest are obtained from arthrographic magnetic resonance images captured before and after surgical treatment. A finite element analysis of a normal hip is also performed for comparison with the pathological case. Physiological loadings and rotational motions are applied. Stresses and contact pressures are evaluated in these patient-specific models in order to better interpret the mechanism of aggression of the femoral and acetabular cartilages and to evaluate the effectiveness of the surgery. The results of the analyses are presented and discussed. The values obtained for the contact pressures in the pathological hip are similar to those reported by other models based on idealised geometries or similar reconstruction methodologies and are larger than the ones obtained in the same hip after the surgical treatment and in the normal hip.

Keywords: hip joint, femoroacetabular impingement, osteoarthritis, femoral cartilage, acetabular cartilage, labrum, 3D reconstruction, finite element method, contact pressure, Von Mises stress.

1 Introduction

The hip joint is unique anatomically and physiologically and is one of the most important joints in the human body. The hip is a classical ball-and-socket joint formed by the femur and the pelvic bone (acetabulum). It is the structural link between the lower extremities and the axial skeleton, transmitting forces from the ground and also carrying forces from the upper extremities and playing a fundamental role in human locomotion [1, 2]. Alterations in the anatomy of this joint, such as femoroacetabular impingement (FAI), can have a great impact in the function of the hip during sports or even routine daily activities and can be a potential cause of human osteoarthritis (OA) [3].

1.1 Femoroacetabular Impingement

Femoroacetabular impingement is a pathology of the hip that is a recognized precursor of joint degeneration. It is characterized by an abnormal morphological relation between the

femoral head and the acetabular cavity that leads to abutment of the femur against the acetabulum during joint motion (mostly flexural and internal rotations) [4]. There are two types of FAI: cam type and pincer type. The cam type is caused by an asphericity in the femoral head (usually located at the anterosuperior quadrant of the region of transition with the anatomical neck) and the pincer type is caused by an abnormal morphology of the acetabulum. The different types of FAI are represented in Figure 1.

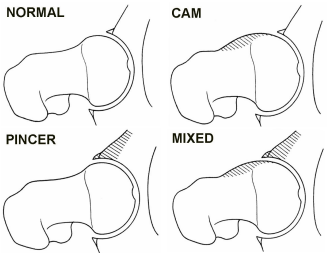

Figure 1: Normal hip and hip with the different types of FAI - cam, pincer and mixed.[5].

The cam type is typically seen in men with ages between 20 and 30 years. The asphericity, which can manifest itself as a flattening of the anterior contour of the femoral head or as an osseous bump, creates a decreased femoral head-neck offset. As the asphericity penetrates into the socket, the cartilages are submitted to a non-physiological (excessive) pressure that can cause macroscopic visible lesions.

At the aspherical femoral head in patients with cam type FAI submitted to surgery, there exists systematically an aspect of increasing fibrillar chondromalacia from the equatorial region to the periphery (Figure 2). These observations are supported by several researchers who found, in the acetabular cartilage of patients with FAI, an increase in the expression of biological markers of OA [6, 7].

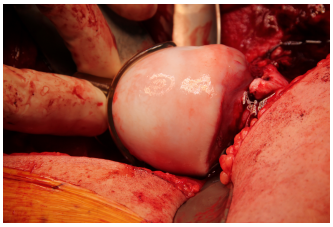

Figure 2: Open surgery that shows the presence of fibrillar chondromalacia on the regions of the deformity.

It is possible to quantify the amount of asphericity of the femoral head using the alpha angle. The alpha angle is the angle between the femoral neck axis and a line connecting the head center with the point where the asphericity begins and it can be measured on radiographs [4]. The upper value for the normal alpha angle is around 42-43^o. With cam FAI there is a decreased femoral head-neck offset which gives rise to an increased value of the alpha angle.

The treatment of the cam type FAI is essentially surgical [8–11] and relies on trimming the head neck junction to remove the non spherical part of the head (osteochondroplasty) .

1.2 Literature Review

Several previous studies report values of the intra-articular pressures in the hip joint. Brown and Shaw [12] reported a peak contact pressure in the hip joint of 8.8 MPa for an applied load of 2700 N. Afoke *et al* [13] measured peak contact pressures varying from 4.9 to 10.2 MPa for applied loads varying from 1980 to 2555 N and a flexural rotation of 27^o. Michaeli *et al* [14] measured peak contact pressures varying from 2 to 8.4 MPa for applied loads varying from 800 to 1200 N. Also von Eisenhart *et al* [15] measured maximum contact pressures in the acetabulum during simulated walking of 6.4 $\pm$ 1.75 MPa at heel strike (for a total applied load of 94% body weight), 7.7 $\pm$ 1.95 MPa at midstance

(345% body weight), 6.4 ± 1.33 MPa at heel-off (223% body weight) and 5.4 ± 1.7 MPa at toe-off (80% body weight). Finally, Anderson *et al*[16] reported experimental pressures ranging from 1.7 to 10.0 MPa during simulated walking, stair climbing and descending stairs.

In the work by Chegini *et al* [17], the authors developed computational models of normal and pathological joints based on variations of the alpha angle and center edge (CE) angle. The alpha angle was varied between 40^o (normal hip) and 80^o (cam FAI) and the CE angle was varied between 0^o (hip dysplasia) and 40^o (pincer FAI). Dynamic loads and motions were applied simulating walking and standing to sitting motion. For a hip with cam FAI (CE angle of 30^o and alpha angle of 80^o) the maximum contact pressure on the acetabular cartilage and labrum was of 12.84 MPa for the standing to sitting motion and 2.35 MPa for walking. The authors concluded that the stresses in the hip joint depend strongly on the geometry of the bony components of the hip and that the pressures are lower for a CE angle between 20^o and 30^o and an alpha angle smaller than 50^o.

In the study by Jorge *et al* [18] the objective was to evaluate the magnitudes of the contact pressures and stresses on the soft components of a hip joint with cam FAI for physiological loading and motion. They used a reconstruction methodology similar to the one used in this paper. The authors used a set of 16 Magnetic resonance imaging (MRI) radial images from a patient with cam FAI with an alpha angle of 98^o and a CE angle of 30^o. For a pure flexural rotation of $90^o$the maximum pressures obtained were of 12-13 MPa for the cartilages and 16 MPa for the labrum. For a pure internal rotation of 24^o maximum pressures of 13-14 MPa for the cartilages and 15 MPa for the labrum were obtained.

2 Reconstruction Methodology

In order to evaluate the order of magnitude of the intra-articular pressures as well as the stresses in the cartilages as a result of the existence of an impingement in the hip, or in a normal hip joint, three cases are analysed.

The 3-D reconstruction methodology is applied to a hip joint of a 21 year-old male patient with a cam-type deformity before and after the surgical treatment and to a normal hip joint (with no deformity) of a 30-year old female patient. Three sets of medical images (one for each case) were provided by a physician, each one composed by a sequence of 24 images.

The initial data set, for the pathological case (alpha angle equal to 90^o), is a set of 24 images that is represented by sequential order in Figure 3. These images were obtained through MRI with the injection of a contrast (intra articular saline solution with Gadolinium) to improve the visualization of the joint components (magnetic ressonance arthrography - MRA). This set of radial images was acquired with a rotation axis coincident with the geometric axis of the femoral neck and containing the centre of rotation of the femoral head. The radial angles of acquisition vary from 0^o to 172.5^o with angular increments of 7.5^o.

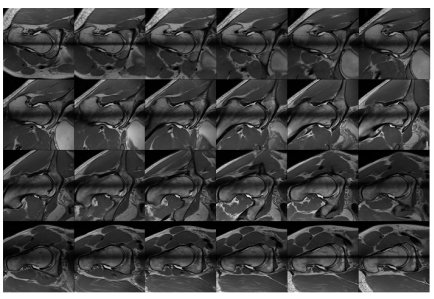

Figure 3: Sequence of MRA images obtained from the patient with cam FAI.

Using Rhinoceros®, the 24 MRA images are manually segmented. This software allows 3D-

modelling and is used for the manual segmentation with spline curves of the medical images [19]. The segmentation allows the extraction of the data relative to the contours that delimit the anatomical structures that constitute the hip joint. In Figure 4, a three-dimensional representation of the 24 acquisition planes, obtained at the end of the segmentation process, can be observed. The figure shows the 24 planes and their position relative to the femur (green) and acetabulum (red).

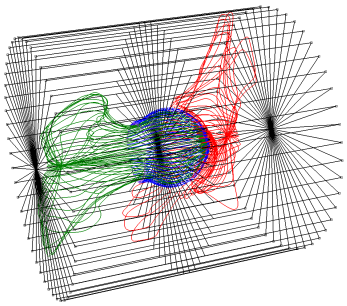

Figure 4: Three-dimensional representation of the 24 acquisition planes in Rhinoceros®.

In order to obtain the 3D reconstruction of the soft structures of the hip joint, a mathematical surface representation of the geometrical data extracted from Rhinoceros® is determined. This is accomplished using an implicit surface interpolation technique based on Radial Basis Functions (RBFs) [18]. Several previous works have shown that RBFs are effective in the reconstruction of medical data [18, 20, 21]. Use is made of the toolbox ® - FastRbf™ (from Fast Field Technology), designed for MATLAB®. The toolbox allows the smooth interpolation of the 3D data (clouds of points) in order to obtain a representation of the surface of interest.The final surfaces obtained using this method are represented in Figure 5.

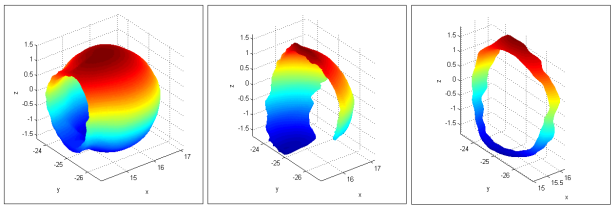

Figure 5: Components of the hip joint (femoral cartilage, acetabular cartilage and labrum) obtained from the three-dimensional reconstruction with RBFs.

The three-dimensional solid models of the anatomical structures are created using SolidWorks® [22]. The 3D solid models, in which the triangular surfaces are interpolated with B-spline cubic patches, are generated and the pieces are combined in order to obtain similar triangular patches in the contact surfaces. The final components of the hip joint are represented in Figure 6.

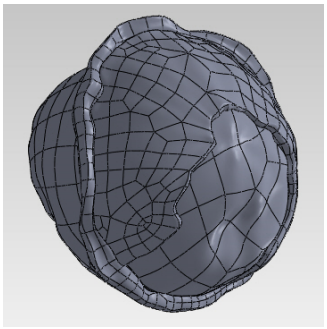

Figure 6: Assembly of the anatomical structures of the pathological hip at the end of the treatment in SolidWorks®.

The solid models obtained using SolidWorks are automatically discretised into finite elements using ABAQUS CAE v.6.9. The Finite Element (FE) mesh of the whole model is represented in Figure 7. The complete mesh of the hip joint contains a total of 270109 tetrahedral linear elements.

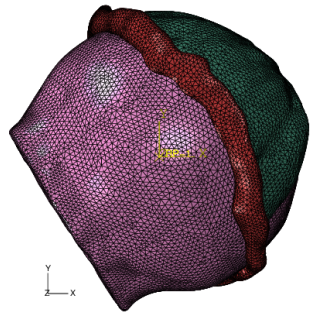

Figure 7: Final finite element mesh of the cam hip model obtained using ABAQUS®. The complete mesh of the hip has a total of 270109 tetrahedral linear elements.

After an arthroscopic femoral osteoplasty with labrum refixation, another set of radial images was acquired. The final FE mesh of the model obtained using a similar reconstruction methodology can be visualized in Figure 8 (a). The complete mesh of the hip has a total of 274074 tetrahedral linear elements. Images of a patient with a normal hip joint (alpha angle equal to 45^o) were also acquired. The FE mesh of the whole model, obtained using again the same reconstruction methodology, is represented in Figure 8 (b). The mesh has a total of 188635 tetrahedral linear elements.

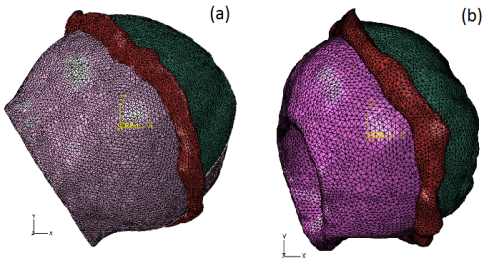

Figure 8: (a) Final finite element mesh of the post-operative hip model obtained using ABAQUS®. The complete mesh of the hip has a total of 274074 tetrahedral elements. (b)Final finite element mesh of the normal hip model obtained using ABAQUS®. The complete mesh of the hip has a total of 188635 tetrahedral linear elements.

3 Results

Previous 2D analyses considering the bony structures as linear elastic or rigid showed practically the same values for the intra-articular pressures [23]. Thus, all the present analyses are performed considering the femur and the acetabulum as rigid bodies. The cartilages and the labrum are considered linear elastic and isotropic. The articular cartilage is a biphasic material with a time-dependent behaviour. However, the loading frequency for normal activities, as walking and sitting, is of the order of 1 Hz, therefore the time-dependent behaviour can be neglected [17]. The articular cartilage has a modulus of elacticity, $E = 12$ MPa [24] and a Poisson ratio of 0.4 [17, 18] and the labrum has a $E = 20$ MPa and a Poisson ratio of 0.4 [17, 18]. These mechanical properties are the same for all the hips analysed in this work. The outer surfaces of the soft tissues in contact with the acetabulum are fixed. All the analyses performed with Abaqus V6.9 are geometrically non-linear. A surface-to surface contact is adopted between the femoral cartilage, as master surface, and the acetabular cartilage and labrum (considered to be tied together), as slave surfaces. The interaction between these two surfaces is considered frictionless and the parameter "finite sliding" is used. Several loading paths are considered. First, the hip joints are subjected only to a physiological compression force in the frontal plane applied at the centroid of the femoral head. With the joints subjected to the compression force, several motions (pure internal and flexural rotations), within the physiological range, are simulated. The three hips analysed in this work are subjected to the same boundary and loading conditions. All the analysis are performed considering that the three patients have a weight of 75 kg (750 N).

The 3 loading paths used in the analyses are:

(a) First, the hip joint is subjected to a compression force with a component of 450 N along the horizontal axis (x-axis) and a component of 1875 N along the vertical axis (y-axis). These values correspond to the maximum force observed during walking and for an individual weight of 750 N [25]. Next, with the joint subjected to this compression force, the effect of a pure internal rotation (about the y-axis) of 45^o is simulated.

b) First, the hip joint is subjected to the compression force of case **a)** and next, with the joint still subjected to this compression force, the effect of a pure flexural rotation (about the x-axis) of 90^o is simulated.

c) First, the hip joint is subjected to a compression force with a component of 225 N along the horizontal axis (x-axis) and a component of 1125 N along the vertical axis (y-axis). These values correspond to the maximum force observed in the standing to sitting motion and for an individual weight of 750 N [25]. Next, with the joint subjected to this compression force, the effect of a pure flexural rotation (about the x-axis) of 90^o is simulated.

During the pure flexural and internal rotations, 11 nodes in the FE mesh of the femoral cartilage of the cam hip are selected, defining straight lines perpendicular to the axis of rotation (Figures 9 and 10). The extremities of these lines are located in the highest and lowest (transition to the cephalic region closest to the neck in the case of the pure flexural rotation or equatorial region in the case of the pure internal rotation) regions of the cam deformity.

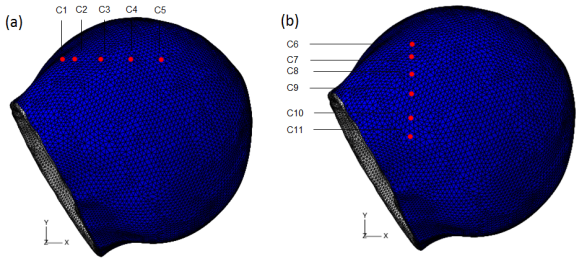

Figure 9: Nodes selected in the FE mesh of the femoral cartilage of the cam hip. (A) Internal rotation - 5 nodes selected numbered from C1 to C5 defining a line perpendicular to the y-axis. (B) Flexural rotation - 6 nodes selected numbered from C6 to C11 defining a line perpendicular to the x-axis.

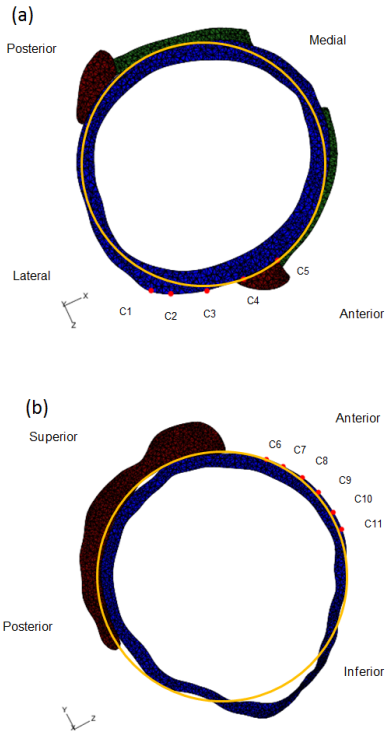

Figure 10: Nodes selected in the FE mesh of the femoral cartilage of the cam hip. (a) Internal rotation - The distance of the nodes to the axis of rotation increases in the direction of the equator of the femoral head. (b) Flexural rotation.

FE analyses of the cam hip after surgical treatment (case 2) and of a non-cam hip (case 3) are also performed for comparison with the pathological case. As in the cam hip model, 11 nodes in the FE mesh of the corresponding femoral cartilage of the patient after surgical treatment, are selected defining straight lines

perpendicular to the axis of flexural rotation (P6 to P11) and to the axis of internal rotation (P1 to P5). For the case of a normal hip morphology, 11 nodes (N1 to N11) from the FE mesh of the femoral cartilage are selected, defining a line perpendicular to the y-axis (internal rotation) and to the x axis (flexural rotation). These nodes are located in regions corresponding to the ones to which the nodes selected in the deformity of the cam hip belong. In Table 1, maximum contact pressures obtained in the pathological case, at the end of each loading path, are presented.

Table 1: Summary of the results obtained for the pathological case at the end of the three loading paths. The maximum values of contact pressure on femoral cartilage (FC), acetabular cartilage (AC) and labrum (L), are represented.

Loading path	**angle of rotation**	**Max. Contact Pressure (MPa)**	
Path a)	40.5^o	FC	12.450
		AC	15.985
		L	15.819
Path b)	90^o	FC	7.114
		AC	10.229
		L	7.080
Path c)	90^o	FC	7.362
		AC	11.442
		L	6.390

A plot, showing the evolution of the contact pressures on the nodes selected perpendicularly to the rotation axis, with the angle of internal rotation, is represented in Figure 11.

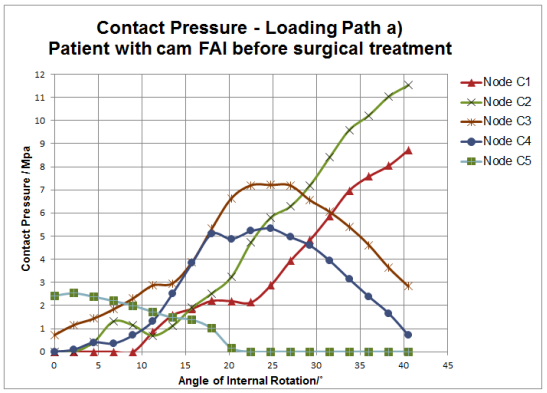

Figure 11: Evolution of the contact pressures during internal rotation of the femur on the nodes selected perpendicularly to the internal rotation axis. The contact pressures vary between 0 and 11.527 MPa (node C2).

The evolution of the contact pressures on the nodes selected perpendicularly to the rotation axiswith the angle of flexural rotation, is represented in Figure 12.

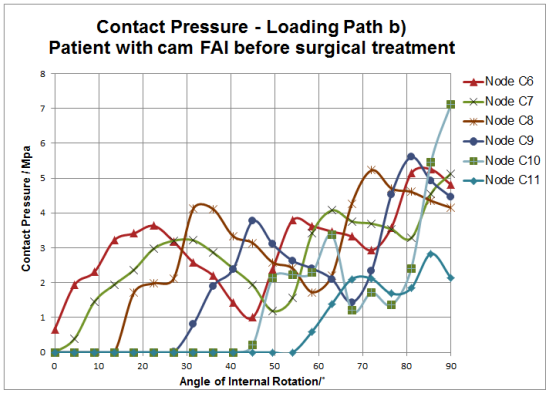

Figure 12: Evolution of the contact pressure during flexural rotation of the femur on the nodes selected perpendicularly to the axis of flexural rotation for loading path b). The pressure varies between 0 and 7.114 MPa (node C10).

The results obtained for the loading path c) are similar to those obtained in loading path b). The plot, showing the evolution of the contact pressure on the selected nodes, with the angle of flexural rotation, is represented in (Figure 13).

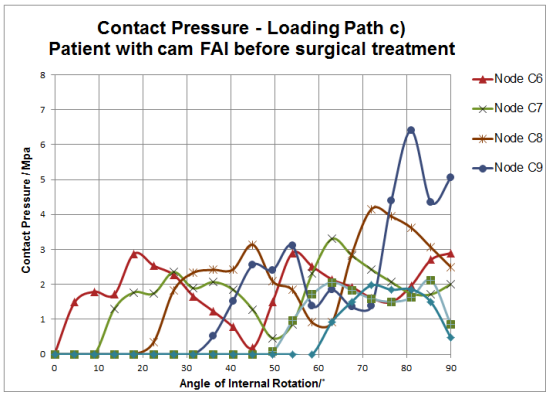

Figure 13: Evolution of the contact pressure during flexural rotation of the femur on the nodes selected perpendicularly to the axis of flexural rotation for loading path c). The pressure varies between 0 and 6.02 MPa (node C9).

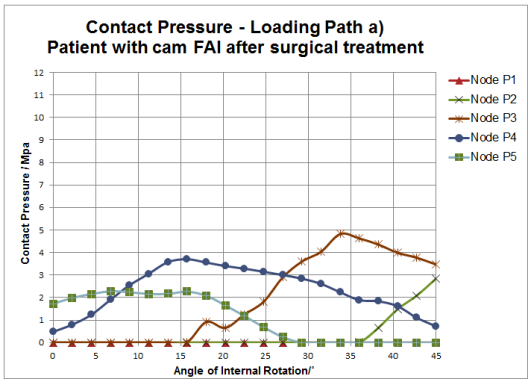

Figure 14: Evolution of the contact pressure during internal rotation of the femur on the nodes selected perpendicularly to the axis of internal rotation. The contact pressure varies between 0 and 4.823 MPa (node P3).

In Table 2, the maximum contact pressures obtained in the postoperative case, at the end of each loading path, are presented.

Table 2: Summary of the results obtained for the postoperative case at the end of the three loading paths. The maximum values of contact pressure on femoral cartilage (FC), acetabular cartilage (AC) and labrum (L), are represented.

Loading Path	angle of rotation	Max. Contact Pressure (MPa)	
Path a)	45^o	FC	10.433
		AC	10.343
		L	11.237
Path b)	90^o	FC	6.816
		AC	7.796
		L	9.976
Path c)	90^o	FC	6.643
		AC	7.275
		L	8.688

The plot showing the evolution of the contact pressure on the points selected perpendicularly to the internal rotation axis with the angle of internal rotation, is represented in Figure 14.

The evolution of the contact pressure on the nodes selected perpendicularly to the rotation axis, with the angle of flexural rotation, is represented in Figure 15.

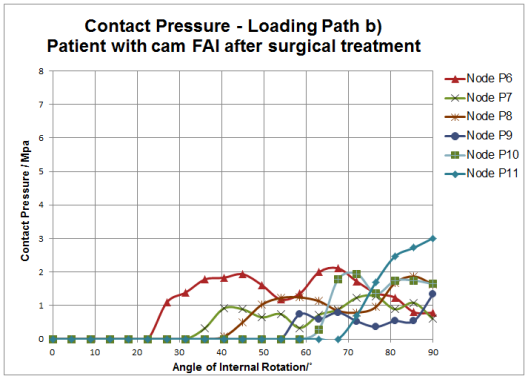

Figure 15: Evolution of the contact pressure during flexural rotation of the femur on the nodes selected perpendicularly to the axis of flexural rotation for loading path b). The magnitudes vary between between 0 and 3.012 MPa (node P11).

The results obtained for loading path c) are similar to those obtained for loading path b). The plot that shows the evolution of the contact pressure on the selected nodes, with the angle of flexural rotation, is represented in Figure 16.

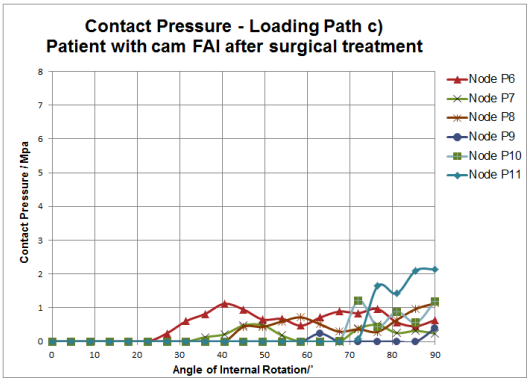

Figure 16: Evolution of the contact pressure during flexural rotation of the femur on the nodes selected perpendicularly to the axis of flexural rotation for loading path c). The pressure varies between 0 and 2.139 MPa (node P11).

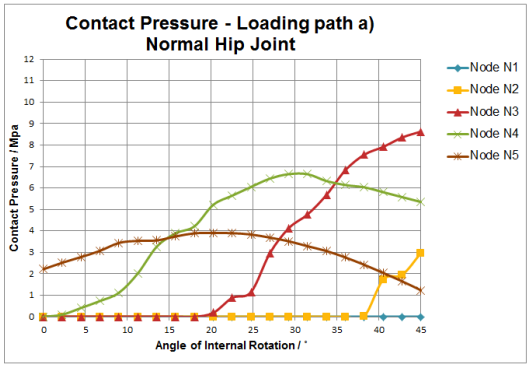

Figure 17: Evolution of the contact pressure during internal rotation of the femur on the nodes selected perpendicularly to the axis of internal rotation. The contact pressure varies between 0 and 8.632 MPa (node N3).

In Table 3, the maximum contact pressures obtained in the normal hip joint at the end of each loading path, are presented.

Table 3: Summary of the results obtained for the normal hip joint at the end of the three loading paths. The maximum values of contact pressure on femoral cartilage (FC), acetabular cartilage (AC) and labrum (L), are represented.

Loading Path	**angle of rotation**	**Max. Contact Pressure (MPa)**	
Path a)	45^o	FC	10.508
		AC	9.383
		L	11.117
Path b)	40.5^o	FC	13.958
		AC	13.574
		L	13.138
Path c)	45^o	FC	13.493
		AC	10.885
		L	16.938

The maximum pressures on the femoral cartilage, acetabular cartilage and labrum for loading paths b) and c) are believed to be artificial and due to reconstruction problems since the analyses stopped before the total rotation was achieved.

The plot showing the evolution of the contact pressure at the nodes selected perpendicularly to the internal rotation axis is represented in Figure 17.

Due to convergence problems the analysis of the loading path b) and of the loading path c) stop when the flexural rotation is equal to 40.5^o and 45^o, respectively. Due to this reason, the contact pressure and the Von Mises stress on the points selected perpendicularly to the flexural rotation axis are not represented.

4 Discussion

The main goals of this thesis are: (1) to contribute to a better understanding and interpretation of the mechanism of aggression of the cartilage in the cam case; (2) to build subject-specific 3D models of the hip joint following reconstruction procedures based on medical images; (3) to perform FE analyses on these 3D models, to evaluate the order of magnitude of pressures at the contact zone and stresses in the cartilages in a cam hip and therefore to establish a correlation with the abnormality and (4) to compare the results with the results obtained in the same cam hip after surgical treatment, in a non-cam hip and in other models so as to validate the analyses and to evaluate the effectiveness of the surgery.

In this study, the FE analyses are performed on models based on the specific anatomy of pa-

tients obtained by reconstruction methodologies and not on totally computer-generated models. The major limitations of the present models are concerned with the physical behaviour of the cartilages which are so far considered linear elastic; also, although less important, the bones are considered rigid; the present models also do not include other tissues present in the hip joint; finally, the manual segmentation performed on the MRA images still is of limited resolution and sometimes it can lead to reconstruction problems.

The rotation movement in the joint seems to be the determinant factor of the origin of high contact pressures in the hips and in particular in the hip with cam-type deformity. The selected movements were chosen to be the more significant in daily activities, namely standing to sitting. This movement implies flexural rotation of the hip joint ranging from 60^o to 90^o.

For an internal rotation movement, comparing the contact pressures in the selected points on the deformity region of the femoral head (Figures 11 and 14) one can observe that in the pathological case the pressures are much higher than in the postoperative case. In the pathological case we can also observe that the contact pressures increase with the distance of the point to the centre of rotation. The nodes located in an area of the femoral head with larger radius of curvature are permanently subjected to a larger and lasting contact pressure than the nodes belonging to the area with smaller radius of curvature. This increase of the contact pressures from the equator of the femoral head to the peripheral regions, where the radius of curvature is larger, seems to be in agreement with the macroscopic lesions observed in the cartilage of patients with cam-type FAI submitted to surgery.

A similar behavior between the pathological and the postoperative cases is observed when a flexural rotation is imposed. Comparing the contact pressures on the selected points on the deformity region of the femoral head (Figures 12 and 15) one can observe that in the pathological case the pressures are much higher than in the postoperative case. In the pathological case the maximum is two times higher. A similar behaviour between the pathological and the postoperative cases is observed when the flexural rotation of loading path c) is imposed.

Comparing now the results obtained in the pathological case with the ones obtained in the normal hip, one observes that, for an internal rotation of the femur, the contact pressures and stresses are lower in the normal hip and closer to the values obtained in the postoperative case. Comparing the contact pressures on the selected points on the deformity region of the femoral head (Figures 11 and 17) one can observe that in the pathological case the pressures are higher than in the normal hip. Comparing now Figures 14 and 17 one can observe that the pressures on the selected points in the postoperative case are lower than the ones obtained in the normal case. That is the pressure on the selected points decreases with the surgery and is even lower than in a normal joint.

Although the results of the analyses depend on a number of factors including joint incongruity, cartilage thickness and material properties, the FE models of the postoperative case and of the normal hip provided predictions for the contact pressures that are in the range of published experimental data on normal hip joints. The FE model of the cam hip also provided predictions for the contact pressures that are in the range of published data obtained on a virtual pathological hip [17] and on a patient specific model of a cam hip obtained using a similar reconstruction methodology [18].

The values obtained for the contact pressures and Von Mises stresses in the pathological hip are larger than the ones obtained in the same hip after the surgical treatment and in the normal hip when an internal rotation is imposed. The values obtained in the postoperative model are even lower than the values obtained in the normal hip model. This seems to indicate that the surgery is really effective in reducing the intra-articular pressures and stresses not only in the region of the deformity but also in all the joint. When a flexural rotation is imposed the values of the contact pressures and stresses obtained in the pathological hip are also larger than the ones obtained after surgery. For this motion, the results obtained in the normal hip model are artificial due to a problem in the reconstruction of the femoral cartilage and could not be compared with the ones obtained in the pathological hip before and after the surgery.

Future developments of the model may include the consideration of the cartilages as porous materials; reconstruction of hip joints including other surrounding tissues like ligaments; consideration of bones as non-rigid; consideration of other imposed forces, motions and more complex boundary conditions. Furthermore, to make the analysis more subject-specific, the material constants of the soft tissues of the patients should be measured and used in the analyses.

References

[1] D. P. Byrne, K. J. Mulhall, and J. F. Baker, "Anatomy & biomechanics of the hip," *Open Sports Medicine Journal*, vol. 4, no. 1, pp. 51–57, 2010.

[2] K. F. Bowman, J. Fox, and J. K. Sekiya, "A clinically relevant review of hip biomechanics," *Arthroscopy: The Journal of Arthroscopic & Related Surgery*, vol. 26, no. 8, pp. 1118–1129, 2010.

[3] R. Ganz, M. Leunig, K. Leunig-Ganz, and W. H. Harris, "The etiology of osteoarthritis of the hip," *Clinical orthopaedics and related research*, vol. 466, no. 2, pp. 264–272, 2008.

[4] O. M. Pena, *Femoroacetabular Impingement*. Springer, 2010.

[5] M. Lavigne, J. Parvizi, M. Beck, K. A. Siebenrock, R. Ganz, and M. Leunig, "Anterior femoroacetabular impingement: part i. techniques of joint preserving surgery," *Clinical orthopaedics and related research*, vol. 418, pp. 61–66, 2004.

[6] M. Leunig, M. Beck, C. Dora, and R. Ganz, "[femoroacetabular impingement: trigger for the development of coxarthrosis]," *Der Orthopade*, vol. 35, no. 1, pp. 77–84, 2006.

[7] S. Wagner, W. Hofstetter, M. Chiquet, P. Mainil-Varlet, E. Stauffer, R. Ganz, and K. Siebenrock, "Early osteoarthritic changes of human femoral head cartilage subsequent to femoro-acetabular impingement," *Osteoarthritis and cartilage*, vol. 11, no. 7, pp. 508–518, 2003.

[8] P. Banerjee and C. R. Mclean, "Femoroacetabular impingement: a review of diagnosis and management," *Current reviews in musculoskeletal medicine*, vol. 4, no. 1, pp. 23–32, 2011.

[9] K. S. Jones, "Arthroscopic femoroplasty in the management of cam-type femoroacetabular impingement," *Clinical orthopaedics and related research*, vol. 467, no. 3, pp. 739–746, 2009.

[10] R. Ganz, T. Gill, E. Gautier, K. Ganz, N. Krügel, and U. Berlemann, "Surgical dislocation of the adult hip a technique with full access to the femoral head and acetabulum without the risk of avascular necrosis," *Journal of Bone & Joint Surgery, British Volume*, vol. 83, no. 8, pp. 1119–1124, 2001.

[11] M. J. Philippon, A. J. Stubbs, M. L. Schenker, R. B. Maxwell, R. Ganz, and M. Leunig, "Arthroscopic management of femoroacetabular impingement osteoplasty technique and literature review," *The American journal of sports medicine*, vol. 35, no. 9, pp. 1571–1580, 2007.

[12] T. D. Brown and D. T. Shaw, "< i> in vitro</i> contact stress distributions in the natural human hip," *Journal of biomechanics*, vol. 16, no. 6, pp. 373–384, 1983.

[13] N. Afoke, P. Byers, and W. Hutton, "Contact pressures in the human hip joint," *Journal of Bone & Joint Surgery, British Volume*, vol. 69, no. 4, pp. 536–541, 1987.

[14] D. A. Michaeli, S. B. Murphy, and J. A. Hipp, "Comparison of predicted and measured contact pressures in normal and dysplastic hips," *Medical engineering & physics*, vol. 19, no. 2, pp. 180–186, 1997.

[15] R. Von Eisenhart, C. Adam, M. Steinlechner, M. Müller-Gerbl, and F. Eckstein, "Quantitative determination of joint incongruity and pressure distribution during simulated gait and cartilage thickness in the human hip joint," *Journal of Orthopaedic Research*, vol. 17, no. 4, pp. 532–539, 1999.

[16] A. E. Anderson, B. J. Ellis, S. A. Maas, C. L. Peters, and J. A. Weiss, "Validation of finite element predictions of cartilage contact pressure in the human hip joint," *Journal of biomechanical engineering*, vol. 130, no. 5, p. 051008, 2008.

[17] S. Chegini, M. Beck, and S. J. Ferguson, "The effects of impingement and dysplasia on stress distributions in the hip joint during sitting and walking: a finite element analysis," *Journal of Orthopaedic Research*, vol. 27, no. 2, pp. 195–201, 2009.

[18] J. Jorge, F. Simões, E. Pires, P. Rego, D. Tavares, D. Lopes, and A. Gaspar, "Finite element simulations of a hip joint with femoroacetabular impingement," *Computer methods in biomechanics and biomedical engineering*, no. ahead-of-print, pp. 1–10, 2012.

[19] *Rhinoceros 4.0 User's Guide.*

[20] J. C. Carr, R. K. Beatson, J. B. Cherrie, T. J. Mitchell, W. R. Fright, B. C. McCallum, and T. R. Evans, "Reconstruction and representation of 3d objects with radial basis functions," in *Proceedings of the 28th annual conference on Computer graphics and interactive techniques*. ACM, 2001, pp. 67–76.

[21] P. Teodoro, P. Pires, J. Martins, and J. Sá da Costa, "Proximal femur parameterization and contact modeling for hip resurfacing surgery," in *3rd Biomechanics National Congress. Proceedings of the 3rd Biomechanics National Congress, Bragança, Portugal*, 2009.

[22] [2011 SolidWorks Help - Scan to 3D; accessed last time 9-October-2013]. [Online]. Available: http://help.solidworks.com/2011/english/SolidWorks/SWHelp_List.html?id=a19de2411be74dcc92d06dcfd1d42249#Pg0

[23] D. Lopes, F. Simões, E. Pires, and P. Rego, "Modelação biomecânica do conflito femuro-acetabular do tipo cam," in *3rd Biomechanics National Congress. Proceedings of the 3rd Biomechanics National Congress, Bragança, Portugal*, 2009.

[24] D. Shepherd and B. Seedhom, "A technique for measuring the compressive modulus of articular cartilage under physiological loading rates with preliminary results," *Proceedings of the Institution of Mechanical Engineers, Part H: Journal of Engineering in Medicine*, vol. 211, no. 2, pp. 155–165, 1997.

[25] G. Bergmann, G. Deuretzbacher, M. Heller, F. Graichen, A. Rohlmann, J. Strauss, and G. Duda, "Hip contact forces and gait patterns from routine activities," *Journal of biomechanics*, vol. 34, no. 7, pp. 859–871, 2001.

FAI femoroacetabular impingement

MRA Magnetic ressonance arthrography

RBFs Radial Basis Functions

CE center edge

FE Finite Element

MRI Magnetic resonance imaging